RESEARCH PAPER

STUDY OF CORROSION MITIGATION OF MILD STEEL IN 3.5% NaCl USING 2-(4-CHLOROPHENYL)-4,5-DIPHENYL-1H-IMIDAZOLE.

Chaitalee Kadam[1*], R. S. Dubey[2]

[1]Department of Chemistry, R.J. College (Autonomous), Ghatkopar (W), Mumbai-400086, India.
ORCID ID: https://orcid.org/0009-0007-1818-5735
[2]Department of Chemistry, R.J. College (Autonomous), Ghatkopar (W), Mumbai-400086, India.
ORCID ID: https://orcid.org/0009-0002-3803-1075

Email ID: chaitaleekadam@rjcollege.edu.in

ABSTRACT

The corrosion inhibitor 2-(4-chlorophenyl)-4,5-diphenyl-1H-imidazole was studied in a 3.5% NaCl solution. The synthesized corrosion inhibitor was studied using gravimetric analysis and thermodynamic and kinetic parameters. The surface morphology of mild steel was studied using scanning electron microscopy and energy-dispersive X-ray analysis. The inhibitor's anti-corrosion property increases with increasing solution concentration. It was studied over the range of 100-600 ppm in the presence of a 3.5% NaCl solution. It shows a maximum inhibition efficiency of 91.89% at 600 ppm. As the solution temperature increased, its inhibitory efficiency decreased. Thermodynamic parameters indicate the electrochemical stability and mixed potential of the metal in a corrosive environment. The activation energy of the inhibitor on the metal surface was studied using kinetic parameters.

Keywords: Weight reduction technique, Anti-corrosive, Imidazole, Mild steel, Inhibition

How to cite this article: Kadam C, Dubey RS. Study of Corrosion Mitigation of Mild Steel in 3.5% NaCl Using 2-(4-Chlorophenyl)-4,5-Diphenyl-1H-Imidazole. Int J Drug Deliv Technol. 2026;16(13s): 848-857. DOI: 10.25258/ijddt.16.13s.93.

INTRODUCTION

Mild steel is widely used in various industries due to its mechanical and chemical properties and low cost. It is used in industrial cooling water pipelines, condensers, and heat exchangers.[1-2] In simulated seawater (3.5% NaCl), chloride ions penetrate and destabilize the passive oxide film on steel surfaces, accelerating uniform, pitting, and localized corrosion. Due to this reduced heat transfer efficiency, leakage and system failure.[3-4] Various techniques have been developed to protect mild steel in chloride solutions, including anodic and cathodic protection and coatings. The most effective method for reducing corrosion is to apply an inhibitor to the metal surface.[5,6]

Organic corrosion inhibitors containing nitrogen, oxygen, and sulfur atoms have been extensively studied for their ability to adsorb onto metal surfaces. Their efficiency depends on structure, electron density, and surface coverage.[7-8] Imidazole derivatives are effective inhibitors of corrosion due to the presence of nitrogen atoms, π-electron conjugation, and strong donor-acceptor interactions with the Fe surface.[9-10] In the present study, 2-(4-chlorophenyl)-4,5-diphenyl-1H-imidazole is highly substituted imidazole derivatives. The combination of diphenyl substitution and chlorophenyl functional group enhances adsorption strength, surface coverage, and inhibition efficiency. The surface morphology of the metal was studied using a scanning electron microscope (SEM) and energy-dispersive X-ray (EDAX) analysis. However, its electrochemical behaviour and thermodynamic adsorption characteristics under cooling-water conditions remain insufficiently explored.

EXPERIMENTAL

*Author for Correspondence: chaitaleekadam@rjcollege.edu.in

Material

Mild steel coupons with dimensions 1 cm*3.5 cm*0.02 cm. These coupons were composed of C-0.16%, Mn-0.40%, Si-0.10%, P-0.013%, and the remaining iron, which were used in all experimental analyses. The mild steel coupons were polished with emery paper no. 60, 80, 100, 150. They were degreased with acetone, then washed with double-distilled water, and dried in a desiccator for further experimental analysis.

Inhibitor and Solution:

An AR grade 35 g of sodium chloride was dissolved in 1 liter of double-distilled water to prepare a 3.5% NaCl solution. The prepared 3.5% NaCl solution was used at different inhibitor concentrations.

Synthesis of inhibitor

A mixture of 0.025 mol benzil, 0.129 mol ammonium acetate, and 0.018mol4-chlorobenzaldehyde in 50ml glacial acetic acid was heated under reflux for 1-2 hours. The reaction mixture was allowed to stand at room temperature. The progress of the reaction was monitored by TLC using ethyl acetate as the eluent. The filtrate was neutralized with ammonium hydroxide to give a solid, which was then filtered. The solid mass obtained from the first and second crops was washed thoroughly with toluene, dried under vacuum, and recrystallized from aqueous ethanol. Yield and melting point were determined.[11]

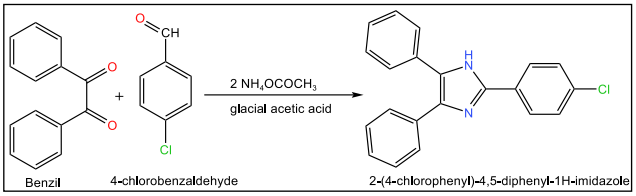

Fig.-1: Synthesis of 2-(4-chlorophenyl)-4,5-diphenyl-1H-imidazole

Weight Reduction Method

The Weight reduction method was carried out in the presence and absence of an inhibitor. The weight reduction analysis was performed by preparing six inhibitor concentrations ranging from 100 ppm to 600 ppm. This experiment was performed at room temperature for 48 hours of immersion and at higher temperatures (308K, 318K, and 328K) for 1 hour of immersion. The mild steel coupons were weighed before immersing in their respective solutions. After their respective times, the metal coupons were washed with acetone and dried in a desiccator. The weights of the mild steel coupons were measured, and the corrosion rate was estimated using equation (1).

$$CR=\frac{W}{S.t} \quad (1)$$

Where CR is the Corrosion rate, W is the difference in the weight of mild steel coupons observed, S is the surface area of mild steel, and t is the immersion time in hours.

The inhibitor efficiency IE (%) was calculated using equation (2).

$$IE\ (\%) = \frac{CR-CR\prime}{CR}\ X\ 100 \quad (2)$$

Where, IE is the inhibition efficiency of corrosion, CR and CR' are the corrosion rates without and with the inhibitor, respectively.

The surface coverage (θ) was calculated by using equation (3).

$$\theta = \frac{CR-CR\prime}{CR} \quad (3)$$

Electrochemical Analysis

Electrochemical analysis of mild steel coupons in 3.5% NaCl was performed by monitoring the open-circuit potential (OCP). It was done using Admiral Instrument electrochemical measuring equipment, the Squidstat Solo 2181, and analyzed in Admiral software. Enamel lacquer was used to coat the mild steel coupons. Uncovered a 1 cm^2 area of the mild steel coupons used to carry the current. The experiment was carried out in a Pyrex glass tank with three electrode necks. The working electrode (a mild steel coupon), reference electrode (a calomel electrode), and counter electrode (a graphite electrode) were immersed in a three-necked flask. Squidstat Solo Instrument was connected to the respective electrodes. The potential was swept from -0.25V to +0.25V at a scan rate of 5mV/s. The open-circuit potentials (OCP) were measured for 60 minutes to obtain a steady-state curve. The potential polarization (PD) curves were obtained for mild steel coupons.

Surface Analysis Technique

The surface morphology of the metal was studied using SEM and EDX, with or without an inhibitor.

RESULTS AND DISCUSSION

Characterization of 2-(4-chlorophenyl)-4,5-diphenyl-1H-imidazole

Characterization of the 2-(4-chlorophenyl)-4,5-diphenyl-1H-imidazole inhibitor was carried out with 'Fourier Transform Infrared Spectrum (FTIR)' in the range of 500-4000 cm^{-1} at a resolution of 2 cm-1 using the Perkin-Elmer 1710 spectrometer. Yield of inhibitor: 80%, Melting Point: 2460 °C-2480 °C, FTIR (KBr cm-1): 732 cm^{-1}(C-H), 1597.5 cm^{-1} (C=N), 3178.65 cm^{-1}(N-H), 1569.75 cm^{-1}(C=C), 640 cm^{-1}(C-Cl).

Weight Reduction Technique

Effect of different concentrations

The weight-reduction technique is used to calculate the corrosion rate and inhibition efficiency, as shown in Table 1. According to this data, the corrosion rate of mild steel decreases, and the inhibitor's inhibition efficiency increases. The inhibitor exhibited maximum inhibition at the optimal concentration. The inhibitor concentration ranged from 100 ppm to 600 ppm; at 600 ppm, the mild steel showed no significant changes in surface appearance. Thus, 600 ppm is the optimal inhibitor concentration for maximum surface coverage. The maximum inhibition efficiency at 600 ppm was 91.89%. The decrease in the corrosion rate in the presence of the inhibitor indicated that the inhibitor molecules adsorbed maximally on the mild steel surface, resulting in minimal corrosion. [12]

Table 1: Weight Reduction Data Obtained for Mild Steel In 3.5% NaCl Solution for Different Concentrations of 2-(4-Chlorophenyl)-4,5-Diphenyl-1H-Imidazole Inhibitor

S. No.	Concentration (ppm)	Corrosion Rate (mgcm-2h-1)	Surface Coverage (θ)	Inhibition Efficiency (IE%)
1	Blank	0.1073	---	---
2	100	0.0055	0.4865	48.65
3	200	0.0261	0.7568	75.68
4	300	0.0174	0.8378	83.78
5	400	0.0145	0.8649	86.49
6	500	0.0116	0.8919	89.19
7	600	0.0087	0.9189	91.89

Effect of temperature

The kinetic parameters were also studied using the 2-(4-Chlorophenyl)-4,5-Diphenyl-1H-Imidazole inhibitor at three elevated temperatures (308 K, 318 K, 328 K) with different concentrations. According to the results in Table 2, inhibition efficiency decreased with increasing temperature. At a higher temperature (328 K), the corrosion rate increased due to increased metal dissolution. Inhibition efficiency decreased with increasing temperature, indicating reduced chemical bonding to the mild steel surface. As a result, the adsorbed inhibitor desorbs from the metal surface and returns to the solution. Thus, forming voids in the protective layer on the metal surface gives rise to pitting corrosion. [12-13]

Table 2: Weight Reduction Data for Mild Steel at Three Temperatures

	Corrosion Rate (mg cm^{-2} h^{-1})			Inhibition Efficiency (IE%)		
Concentration (ppm)	308 K	318 K	328 K	308 K	318 K	328 K
Blank	0.1102	0.1131	0.1160			
100	0.0580	0.0609	0.0638	47.37	46.15	45
200	0.0290	0.0319	0.0348	73.68	71.79	70
300	0.0203	0.0232	0.02611	81.58	79.49	77.5
400	0.0174	0.0203	0.02321	84.21	82.05	80

500	0.0145	0.0174	0.02031	86.84	84.61	82.5
600	0.0116	0.0145	0.01740	89.47	87.18	85

Activation Parameters

The effect of temperature on the surface of mild steel can be explained by using the following Arrhenius equation.

$$\ln C.R. = \ln A \frac{Ea}{RT}$$

The ln CR versus 1/T plot suggested that the activation energy was calculated from the slope of the plot (Fig.). From the data in Table 3, it is observed that the activation energy is low for the uninhibited mild steel coupon, whereas it is higher for the inhibited mild steel coupon. As the inhibitor concentration increases, the activation value increases as well. The higher activation value Where CR is the corrosion rate calculated from the weight loss of mild steel, A is the Arrhenius pre-exponential factor, Ea is the activation energy from the corrosion process, R is the universal gas constant, and T is the absolute temperature (K).

indicates that the inhibitor formed a protective film on the mild steel coupon surface, acting as an energy barrier between the saline solution and the surface.[12,14]

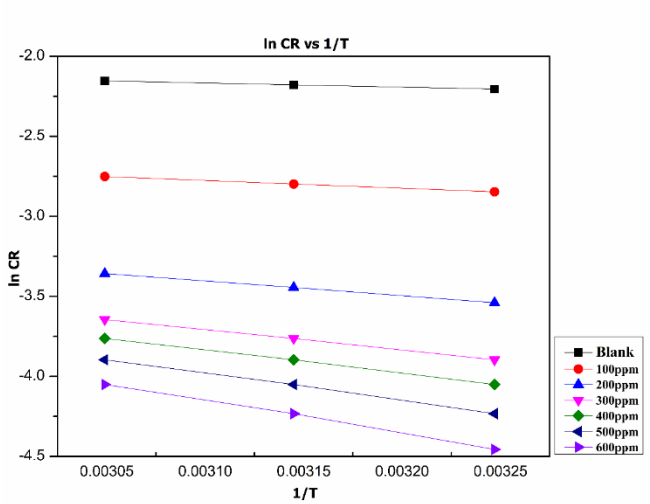

Fig. 2: Arrhenius Plot of Mild Steel Corrosion in Saline Solution with and Without Different Concentrations of Imidazole Derivative Inhibitor.

Table 3: Activation parameters of mild steel in the presence of the studied inhibitor

S. No.	Concentration (ppm)	R^2	Ea (kJ/mol)	ΔH (kJ/mol)	-ΔS (J/mol)	ΔG			
						298 K	308 K	318 K	328 K
1	0	0.998	2.23	0.41	265	79	82	84	87
2	100	0.989	4.13	1.5	263	78	81	83	86
3	200	0.999	8	5.3	257	77	79	82	84
4	300	0.989	11.	8.4	250	75	77	80	82
5	400	0.969	13	10	246	73	75	78	80
6	500	0.991	15	12.35	240	71	74	76	78
7	600	0.998	19	17	228	68	70	72	74

The following equations are used to calculate the enthalpy of activation (ΔH) and entropy of activation (ΔS)

$$C.R = \frac{RT}{Nh} exp\left[\frac{\Delta S}{R}\right] exp\left[-\frac{\Delta H}{RT}\right]$$

Where (ΔH) is the enthalpy of activation, (ΔS) is the entropy of activation, h is Planck's

constant, R is the universal gas constant, N is Avogadro's Constant, and T is the absolute temperature. Figure- showed the transition state of the investigated inhibitor and blank saline solution on mild steel coupons. The value of enthalpy activation and the enthalpy of entropy are derived from the slope and y-intercept of the graph. From the data in Table 3, ΔH is positive and increases with increasing inhibitor concentration. These positive values indicated that metal dissolution occurs slowly due to the presence of an inhibitor. The 2-(4-chlorophenyl)-4,5-diphenyl-1H-imidazole inhibitor formed a protective film on the metal surface. The negative, increasing value of ΔS indicated an increase in entropy upon formation of the activated complex.[15-17]

The Gibbs free energy of activation was introduced using the following equation:

$$\Delta G = \Delta H - T\Delta S$$

The change in Gibbs free energy showed the spontaneity of corrosion on the surface of the mild steel. At higher temperatures, the corrosion process becomes spontaneous, and the inhibitor desorbs, thereby reducing the protective barrier on the mild steel surface and increasing ΔG.[18-19]

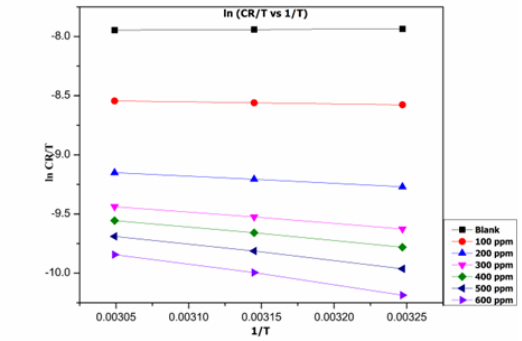

Fig. 3: transition state plots for the mild steel coupons in the presence and absence of the investigated inhibitor

Adsorption Isotherms

Organic inhibitor 2-(4-Chlorophenyl)-4,5-Diphenyl-1H-Imidazole showed an adsorption mechanism on the active site of the mild steel coupons. To understand the interaction between the mild steel surface and the inhibitor. Various adsorption isotherms, including the Langmuir, the Freundlich, and the Temkin, were plotted, but the Langmuir isotherm provided the best fit. It is calculated from the equation given below:

$$\frac{C}{\theta} = \frac{1}{\text{Kads}} + C$$

Where C is the concentration of organic heterocyclic compound as inhibitor, Kads is the adsorptive equilibrium constant, and θ is the surface coverage. It is observed that Figure 4 shows linearity, with a linear regression coefficient (R^2) and slope values close to unity, as listed in Table 4. The organic inhibitor formed a uniform monolayer on the metal surface, protecting it from corrosion.[20]

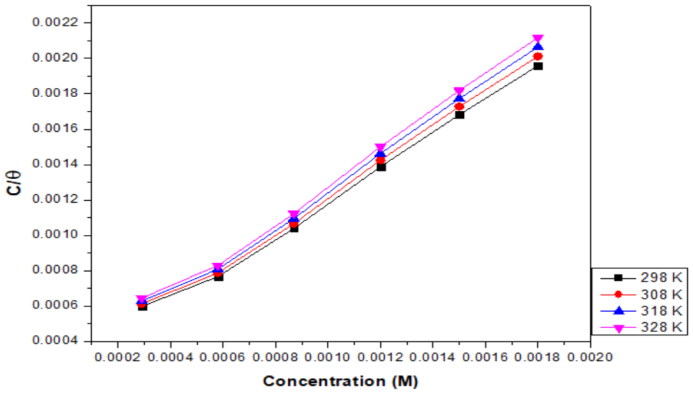

Fig. 4: Adsorption plots of MS coupons in saline solution at different temperatures

The Kads are calculated from the y-intercept. It was observed that the adsorptive equilibrium constant Kads decreased with increasing temperature. The value of Kads indicates the inhibitor's adherence to the metal surface. The lower Kads value indicated weak adherence due to the inhibitor dissolving back into the solution.[21-22]

The standard free energy of adsorption can be calculated by using equation no. (8).

$$(\Delta G^0_{ads}) = -RT \ln (55.5\ \text{Kads})$$

The negative value of (ΔG^0_{ads}) indicated spontaneous adsorption of the investigated inhibitor. R is the universal gas constant, T is thermodynamic temperature, and the value of 55.5 indicates the molar concentration of water in the solution. ΔG^0_{ads} gives the information on the adsorption of the inhibitor on the metal surface. The studied organic inhibitor shows physisorption or chemisorption with the mild steel surface. If the value of ΔG^0_{ads} is greater than -20 kJ/mol, then physical adsorption occurs. If the value is greater than -40kJ/mol, then chemical adsorption is

observed. Physisorption occurs when an inhibitor molecule donates a lone pair of electrons to an iron surface with a vacant d-orbital. Chemisorption occurs when a covalent bond is formed between the charged portion of the organic inhibitor and the surface of the metal. Table 4 indicates that the inhibitor exhibits both physical and chemical adsorption on the surface of mild steel.[23-24]

The adsorption enthalpy (ΔH^0_{ads}) and adsorption entropy (ΔS^0_{ads}) were calculated by using the Van't Hoff equation. The obtained values are listed in Table 4.

$$\ln Kads = - \frac{\Delta H° ads}{RT} + \frac{\Delta S° ads}{R} + \ln \frac{1}{55.5}$$

Table-4: Thermodynamic Adsorption Parameters of 2-(4-Chlorophenyl)-4,5-Diphenyl-1H-Imidazole at different temperatures

S. No.	Temperature (K)	R^2	Slope	Kads	$-\Delta G^0_{ads}$ (kJ/mol)	ΔH^0_{ads} (kJ/mol)	$-\Delta S^0_{ads}$ (J/mol)
1	298	0.979	0.932	3722	30.32	2.14	136.28
2	308	0.999	0.952	3624	31.27		
3	318	0.994	0.983	3530	32.22		
4	328	0.969	1.008	3443	33.16		

From Figure 5, ΔH^0_{ads} and ΔS^0_{ads} are calculated from the slope and intercept of the graph, respectively. The negative ΔH^0_{ads} value indicated a spontaneous exothermic adsorption process, which accounts for low inhibition efficiency at high temperature. The positive ΔS^0_{ads} value indicated that the system's entropy increased during adsorption due to the desorption of water molecules. [25-26]

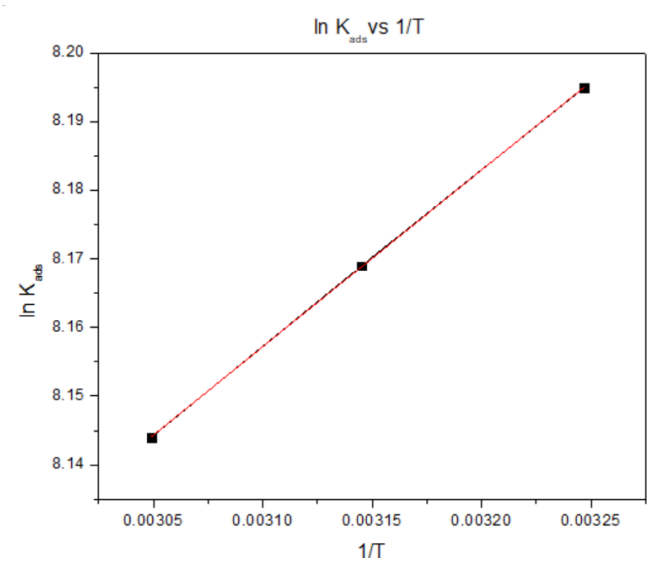

Fig. 5: Van't Hoff Plot of Mild Steel in saline solution

Electrochemical Analysis

Open Circuit Potential (OCP) measurement

The open-circuit potential of mild steel was measured in the presence and absence of the inhibitor under study. The curves obtained at different concentrations indicate a potential shift towards the positive side. The uninhibited solution shifts towards the negative side. In addition to more inhibitors, a steady potential is achieved. Due to the presence of an organic inhibitor, potential shifts toward the more positive side affected the anodic part of the reaction on mild steel. This demonstrated that the inhibitor was successfully adsorbed on the metal surface and formed a protective coating.[27]

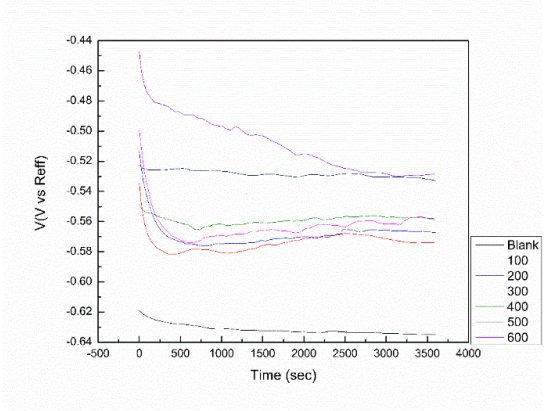

Figure 6: Open Circuit potential Curves for mild steel in the saline solution with and without the studied inhibitor 2-(4-chlorophenyl)-4,5-diphenyl-1H-imidazole in 3.5% NaCl solution.

Potentiodynamic Polarization measurement

Potentiodynamic polarization measurements were performed at inhibitor concentrations ranging from 100 ppm to 600 ppm. The electrochemical parameters include (Ecorr) corrosion potential, (Icorr) corrosion current densities, (βa) the Tafel slope of an anode, (βc) the Tafel slope of the cathode, and Inhibition efficiency (IE%). The inhibition efficiency is computed using the following equation:

$$IE\% = \frac{icorr - icorr'}{icorr} X\ 100$$

Where, i_{corr} is the corrosion current density of uninhibited mild steel, and i_{corr}' is the corrosion current density in the presence of the inhibitor. The shift of Ecorr towards a more positive side, as compared to an uninhibited mild steel coupon, suggests that the inhibitor is capable of obstructing both the anodic and cathodic reactions. As the inhibitor concentration increases, the corrosion inhibition efficiency increases, reaching a maximum of 94.5% at 600 ppm.

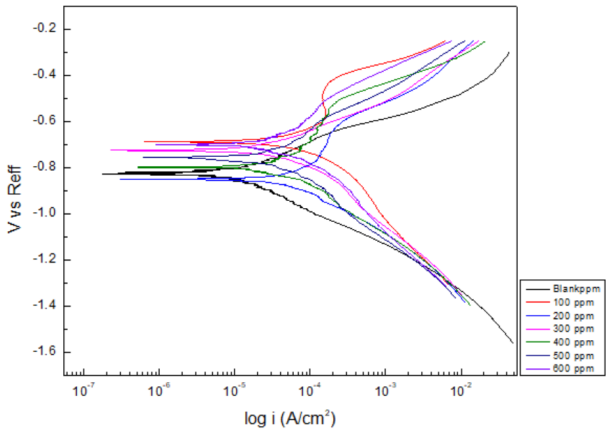

Figure 7 Potentiodynamic polarization curves of mild steel in saline solution with and without inhibitor

Table 5: Potentiodynamic Polarization Parameters for the Corrosion of Mild Steel in 0.1 N HCl without and with different Concentrations of 2-(4-chlorophenyl)-4,5-diphenyl-1H-imidazole.

S. No.	Concentration (ppm)	-Ecorr (mv)	Icorr (μA)	βa 10-3 (V/dec)	βc 10-3 (V/dec)	IE %	Corrosion rate (mpy)
1	Blank	643	200	148	384		91.41
2	100	507	102	142	251	49	46.89
3	200	226	46.6	68.9	197	76.7	21.35
4	300	484	39.2	93.1	267	80.4	17.93
5	400	589	25.3	147	184	87.35	11.58
6	500	539	18.6	26.8	164	90.7	8.51
7	600	392	11	12.8	83.8	94.5	5.04

According to the literature, if the difference in Ecorr values between the inhibited and blank solutions exceeds 85 mV, the inhibitor is classified as cathodic or anodic. In the current study, the largest difference in Ecorr was 25 mV, indicating that the inhibitor exhibits mixed adsorption. The employed inhibitor is adsorbed on the surface of mild steel, inhibiting processes occurring at the anode and cathode. Furthermore, no changes are detected in the cathodic and anodic curves.[27-28]

Surface Analysis

Scanning Electron Microscope (SEM)

The surface morphology of the mild steel was studied in the presence and absence of an organic heterocyclic inhibitor in a saline solution. An organic inhibitor at a higher concentration of 600 ppm was investigated by using a scanning electron microscope. Figure 8A depicts the SEM of a mild steel surface before immersing in a saline solution. Figure 8 B shows the SEM image of the mild steel surface after 48 hours in saline solution. Figure 8C illustrates the Sem image of a mild steel surface after immersion in saline solution in the presence of 600 ppm inhibitor concentration for 48 hours.

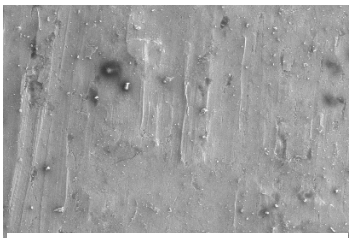

Fig. 8(A)

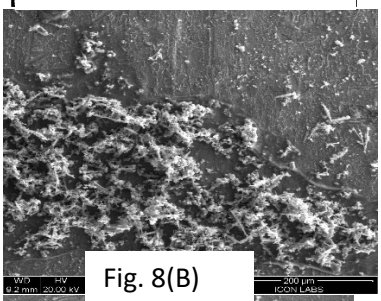

Fig. 8(B)

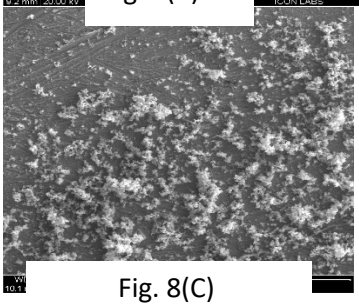

Fig. 8(C)

Fig 8A image before immersion shows a smooth surface, with no cracks or pitting corrosion observed. Fig. 8B pitting corrosion and cracks formed on the surface of the metal. This indicates that in the presence of a saline solution, the mild steel surface undergoes destruction. The plain surface with some cracks was obtained in the presence of the investigated inhibitor. hence proved an organic heterocyclic inhibitor successfully employed on the surface of MS coupons to give protection against a saline medium. [29]

EDAX Analysis Technique

The EDAX technique is used to detect the elements present in mild steel coupons. Figures 9A and 9B show the spectra obtained in the presence of a saline solution and a high-concentration (600 ppm) inhibitor solution. The spectra of 9 indicate the presence of the functional group in the heterocyclic organic inhibitor. [29]

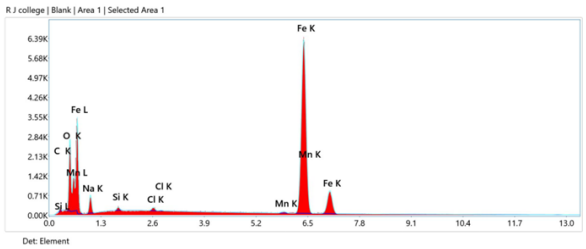

Fig.9(A) EDAX Spectra for Mild Steel After Immersion in 3.5% NaCl Solution for 48 Hours

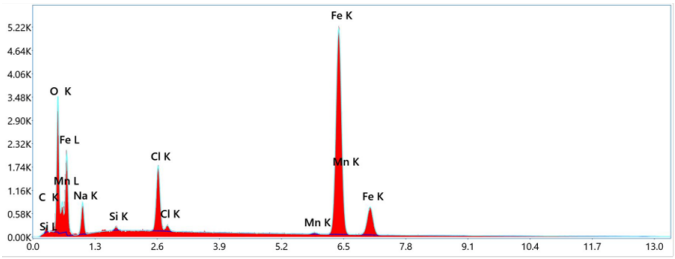

Fig.9(B) EDAX Spectra for Mild Steel in the Presence of 600 Ppm of Studied Inhibitor

Adsorption mechanism of inhibitor:

The present is an organic inhibitor studied in a saline environment, attributed to strong adsorption on the metal surface.

In the presence of 3.5% NaCl solution:

Mild steel undergoes anodic dissolution:

$$Fe^{2+} + 2e^- \longrightarrow Fe$$

Oxygen reduction at the cathodic reaction:

$$O_2 + 2H_2O + 4e^- \longrightarrow 4OH^-$$

Chloride ions (Cl^-) accelerate corrosion and dissolution of metal. It is a more electronegative element. The imidazole ring, which contains two nitrogen atoms, has high electron density. And it's a π-electron-rich system. It acts as a mixture of physisorption and chemisorption. Cl^- adsorb on the positively charged surface of mild steel and create a negatively charged layer. This is a physisorption process. Protonated imidazole blocks the active corrosion site on the mild steel surface. The nitrogen atom donates lone-pair electrons to the vacant d-orbitals of Fe and forms a coordinate covalent bond. This is a chemisorption process. Surface coverage via mixed adsorption involving electrostatic interaction and coordinate bonding

through nitrogen atoms and aromatic π-electrons, forming a compact protective film that blocks both anodic metal dissolution and cathodic oxygen reduction reactions. Due to the presence of an organic heterocyclic inhibitor, the corrosion rate decreases significantly. 12,30

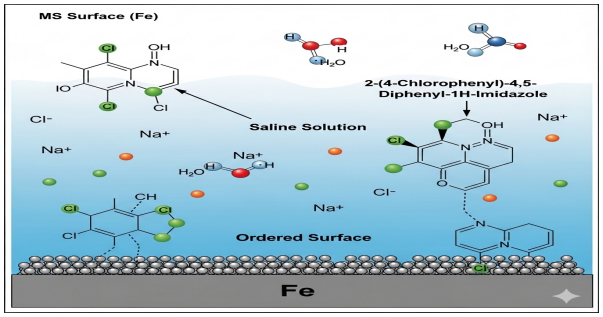

Fig. 10: Corrosion Inhibition Mechanism of 2-(4-Chlorophenyl)-4,5-Diphenyl-1H-Imidazole

CONCLUSION

The2-(4-Chlorophenyl)-4,5-Diphenyl-1H-Imidazole derivative of imidazole was synthesized, and its characteristics and properties were studied using FTIR. The weight reduction analysis indicates good inhibition efficiency, as evidenced by a decrease in the corrosion rate. As the solution temperature increased, inhibition efficiency decreased, and the inhibitor desorbed. Based on data from the above electrochemical techniques, potentiodynamic polarization, and surface morphology of the mild steel, it is concluded that the investigated inhibitor exhibits mixed-type adsorption, indicating a spontaneous reaction on the mild steel surface. It obeys the Langmuir adsorption isotherm, which supports the formation of a protective monolayer of inhibitor on the surface of mild steel. The adsorption of the MS on the metal surface, as detected by SEM and EDAX images, indicates successful adsorption.

ACKNOWLEDGMENTS

The authors are grateful to the authorities of their institutions for their cooperation and support.

CONFLICT OF INTERESTS

The authors declare there is no conflict of interest.

AUTHOR CONTRIBUTIONS

All the authors contributed significantly to this manuscript, participated in reviewing/editing, and approved the final draft for publication. The research profile of the authors can be verified from their ORCID IDs, given below:

Chaitalee Kadam https://orcid.org/0009-0007-1818-5735

R.S. Dubey https://orcid.org/0009-0002-3803-1075

REFERNCES

1. O.S.I.Fayomi, A. P. I. Popoola, Journal of Physics, 1378, 1, (2019), 10.1088/1742-6596/1378/2/022006
2. F. Afshari, E. R. Ghomi, M. Dinari, S. Ramakrishna, Chemistry Select, 8(9), e202203231(2023), https://doi.org/10.1002/slct.202203231
3. K. Muthamma, P. Kumari, M. Lavanya, S. A. Rao, Journal of Bio- and Tribo-Corrosion 7, 10(2020), https://doi.org/10.1007/s40735-020-00439-7
4. P. Raotole, R. S. Khadayte, V. Huse, International Journal of Creative Research Thoughts (IJCRT), 10 (12), 1, (2022).
5. J, Jain, Iranian Journal of Chemical Engineering, 41, 3365 (2021).
6. J. Ken, B. Balangao, Journal of Chemical Health Risks, 14 (1), 79-87, (2024).
7. Yu. I. Kuznetsov, International Journal of Corrosion Scale Inhibitors, 1, 15, (2012), http://dx.doi.org/10.17675/2305-6894-2012-1-1-003-015
8. H. M. Yang, Molecules, 26 (11), 3473, (2021), https://doi.org/10.3390/molecules26113473
9. M. Ouakki, H. Chahmout, Journal of Molecular Liquids, 433, 1, (2025), https://doi.org/10.1016/j.molliq.2025.127922
10. K. Dahmani, Z. Aribou, Colloids and Surfaces A: Physicochemical and Engineering Aspects, 704, (2025),

https://doi.org/10.1016/j.colsurfa.2024.135376
11. A. Puratchikody, S. Gopalkrishnan, Indian Journal Pharma Science, 67(6), 725-731, (2005).
12. C. Verma, M. A. Quraishi, Ain Shams Engineering Journal, 7(1),1(2016), https://doi.org/10.1016/j.asej.2015.11.017
13. K. Haruna, O. Charles , Heliyon, 10 (19), e38116, (2024), https://doi.org/10.1016/j.heliyon.2024.e38116.
14. N. Timoudan, Arej S. Al-Gorair, Royal Society of Chemistry, 14, 30295-30316, (2024), https://doi.org/10.1039/D4RA05070C
15. D. Karra, N. Timoudan, International Journal of Electrochemical Science, 20 (5), 100978, (2025), https://doi.org/10.1016/j.ijoes.2025.100978
16. A. A. Adamu, O.R. A. Iyun, BMC Chemistry, 19 (163), (2025), 10.1186/s13065-025-01541-y
17. M. E. Azhar, B. Mernari, M. Traisnel, F. Bentiss, M. Lagrenée, Corrosion Science, 43, 2229(2001), https://doi.org/10.1016/s0010-938x(01)00034-8
18. Ana I.M.C. L. Ferreira, M. A. V. R. D. Silva, Journal of Chemical Thermodynamics, 48, 84-92, (2012), 10.1016/j.jct.2011.12.001
19. B. Chaugh, A. K. Singh, S. Thakur, American Chemical Society, 5(22), 1, (2020), 10.1021/acsomega.9b04274
20. A. Kokalj, Corrosion Science, 217, 1111112, (2023), 10.1016/S0010-938X(00)00053-1
21. L. Gao, S. Peng, Royal Society of Chemistry, 8, 38506, (2018), 10.1039/C8RA06145A
22. A. Y. Musa, A.B. Mohamad, Journal of Central South University, 17, 34-39, (2010), 10.1007/s11771-010-0007-5
23. H. Jafari, I. Danaee, American Chemical Society, 52, 6617-6632, (2013), 10.1021/ie400066x
24. M. V. Putz, C. G. Vaszilcsin, Journal of Molecular Structure, 1286, 135643, (2023), 10.1016/S0010-938X(00)00053-1
25. P. Kamble, R. S. Dubey, International Journal of Scientific Research in Science, Engineering and Technology, 5(4), 95(2018).
26. C. R. Girish, Chemical Papers, 79, 5687-5706, (2025), 10.1007/s11696-025-04218-x
27. Y. Qiang, S. Zhang, and S. Chen, Corrosion Science, 119, 68-78, (2017) 10.1016/j.corsci.2017.02.021
28. S., M.A. Quraishi, Corros. Sci. 70 ,161-169, (2013), 10.1016/j.corsci.2013.01.025
29. M.D.Weeks, R.Subramanian, Surface Coating And Technology, 273, 50-59, (2015), 10.1016/j.surfcoat.2015.02.012
30. W. Daoudi, A. Chaouiki, Journal of Taiban University of Science, 18 (1), (2024), https://doi.org/10.1080/16583655.2024.2377305